PYRITE DISSOLUTION IN ACIDIC MEDIA

DESCOSTES, M.*, VITORGE P(1). AND BEAUCAIRE, C.(2)

CEA, DEN Saclay, DPC/SECR/L3MR, CEN, F-91191 Gif-sur-Yvette, France.

* Author to whom correspondence should be addressed (michael.descostes@cea.fr).
(1) CEA, DEN Saclay, DPC/SECR/L3MR and UMR 8587 (CEA, Evry University, CNRS).
(2) Present address: IRSN/DPRE/SERGD, F-92265 Fontenay-aux-Roses, France.

Date de révision : 07/07/2003 00:21:00

ABSTRACT

Oxydation of pyrite (initially free from oxidation products) by atmospheric oxygen (20%) in aqueous solutions was studied at 25℃ usin g short-term batch experiments. Fe^{2+} and SO_4^{2-} were the only dissolved Fe and S species detected in these solutions. After a short period, $R = [S]_{tot}/[Fe]_{tot}$ stabilized from 1.25 at pH = 1.5 to 1.6 at pH = 3. These R values were found to be consistent with previously published measurements (as calculated from the raw published data). This corresponds to a non stoichiometric dissolution ($R < 2$) inherited from an aqueous sulphur deficit. Thermodynamics indicate that S(-I) oxidation can only produce $S^0_{(s)}$ and SO_4^{2-} in the above equilibrium conditions. However, calculation of Pourbaix diagrams assuming the absence of SO_4^{2-} indicate that $S_2O_3^{2-}$ and $S_4O_6^{2-}$ can appear in our experimental conditions. Using these species the simplest expected oxidation mechanism is

$FeS_{2(s)} + 1.5\ O_2 \rightarrow Fe^{2+} + S_2O_3^{2-}$
followed by

$S_2O_3^{2-} + 1.2\ H^+ \rightarrow 0.4\ S^0_{(s)} + 0.4\ S_4O_6^{2-} + 0.6\ H_2O$,
and finally

$S_4O_6^{2-} + 3.5\ O_2 + 3\ H_2O \rightarrow 4\ SO_4^{2-} + 6\ H^+$
possibly in several steps.

The overall reaction is
$FeS_2 + 2.9\ O_2 + 0.6\ H_2O \rightarrow Fe^{2+} + 0.4\ S^0_{(s)} + 1.6\ SO_4^{2-} + 1.2\ H^+$,

consistent with R = 1.6. In the most acidic (pH = 1.5) conditions, SO_2 formation is expected as an intermediary step of the oxidation of $S_4O_6^{2-}$ to SO_4^{2-}. Exsolution of $SO_{2(g)}$ would result in R values smaller than 1.6, again consistent with experimental observations. The above multistep mechanism, based on known aqueous redox chemistry of sulphur species can account for the deficit in aqueous sulphur noticed in all published experimental observations. $S_2O_3^{2-}$ is assumed to be the product of the first dissolution step of FeS_2. In a second step $S_2O_3^{2-}$ disproportionates into $S^0_{(s)}$ and a metastable sulphoxyanion further oxidised to SO_4^{2-}. The intermediary species usually could not be detected in this study, consistent with calculated concentrations

below the detection limit under acidic conditions. Under non-acidic conditions, the $S_2O_3^{2-}$ species could be detected, but correct evaluation of the dissolution mechanism is hindered by precipitation of Fe(III) as iron oxyhydroxydes.

1. INTRODUCTION

Pyrite (FeS_2) is one of the main minerals on Earth, participating in the sulphur and iron global cycle on geosphere. Pyrite is known as a redox buffer in anoxic conditions (Beaucaire *et al.*, 2000), and therefore as a redox sink for sulphur and iron since its solubility is very low (Berner, 1984). Its presence, hence synonymous of reducing conditions, is often used as an indicator of uranium and metal hydrothermal ores in geochemical exploration (Rich *et al.*, 1977). The surface reactivity of pyrite is often mentioned through origin of life (McClendon, 1999; Wächtershäuser, 2000), sorption of precious metals Au and Ag (Scaini *et al.*, 1997), and is studied as a cellular solar energy (Ennaoui *et al.*, 1986). Finally, pyrite exposed to oxygen or another oxidant can oxidize according to

$$FeS_2 + 7/2\ O_2 + H_2O \rightarrow Fe^{2+} + 2\ SO_4^{2-} + 2\ H^+, \qquad (1)$$

leading to the release of two moles of H^+ per mole of oxidized pyrite. Acidification can be enhanced by the oxidation of iron according to

$$FeS_2 + 15/4\ O_2 + 7/2\ H_2O \rightarrow Fe(OH)_{3(s)} + 2\ SO_4^{2-} + 4\ H^+ . \qquad (2)$$

However, in more acidic conditions, ferric iron, produced in reaction (2), is also known as a strong oxidant of pyrite (Garrels and Thomson, 1960; Moses *et al.*, 1987; Singer and Stumm, 1970). This oxydation autocatalysis can be written

$$FeS_2 + 14\ Fe^{3+} + 8\ H_2O \rightarrow 15\ Fe^{2+} + 2\ SO_4^{2-} + 16\ H^+ . \qquad (3)$$

Reactions (1-3) described process occurring upon acid mine drainage as well documented down stream of sulphur ores mining (see for example the Doñana ecological disaster in Spain, Pain *et al.*, 1998; or Evangelou, 1995).

FeS_2 oxidative dissolution has been studied using most analysis techniques available to scientists, such as electrochemistry (Bailey and Peters, 1976; Biegler and Swift, 1979; Wei and Osseare, 1997), solution chemistry (Kamei and Ohmoto, 2000; McKibben and Barnes, 1986; Nicholson *et al.*, 1988 and 1990), spectroscopic techniques (Descostes *et al.*, 2002a; Donato *et al.*, 1993; Knipe *et al.*, 1995) and others techniques (Descostes *et al.*, 2001; Fornasiero *et al.*, 1992; McGuirre *et al.*, 2001; Taylor *et al.*, 1984). Recently, synchrotron X-ray photon electron spectroscopy surface (Guevremont *et al.*, 1998; Nesbitt *et al.*, 2000; Schaufus *et al.*, 1998; Uhlig *et al.*, 2001) and near-field microscopy under ultra-high vacuum (Rosso *et al.*, 1999a, b) were also used to investigate the pyrite surface at an atomic scale. Despite all these efforts, no consensus emerges on a single and well-established oxidation mechanism.

Recent literature focuses on acidic dissolution observed by spectroscopic techniques. Sasaki *et al.* (1995) observed a sulphur rich layer on pyrite surface oxidized in ferric medium ($FeCl_3.6H_2O$ 15 mmol L^{-1}) at pH = 2 during 72 hours. These authors concluded to a non-stoichiometric oxidation of pyrite with a preferential dissolution of iron, as also proposed by several other studies (Mycroft *et al.*, 1990;

Bonnissel-Gissenger *et al.*, 1998; McGuirre *et al.*, 2001; Ahlberg and Broo, 1997; Bucley and Woods, 1987; Toniazzo *et al.*, 1999; Zhu *et al.*, 1994). Nevertheless, Luther (1997) argued that their interpretation was erroneous (see also Sasaki *et al.*, 1997), based on his mechanism proposed earlier from electronic orbital considerations (Luther, 1987) and sulphur aqueous chemistry. Luther (1997) proposed that the sulphur rich layer on pyrite surface is not a direct oxidation product, but should stem from the disproportion of thiosulphate ($S_2O_3^{2-}$), the actual oxidation product of pyrite, into elementary sulphur (S_8 or S^0) and hydrogenosulphite (HSO_3^-) according to:

$$8\ S_2O_3^{2-} + 8\ H^+ \rightarrow S_8 + 8\ HSO_3^- \qquad (4)$$

The sulphur superficial enrichment of the oxidized pyrite surface analysed by Sasaki *et al.* (1995) would therefore result not from non-stoichiometric dissolution with iron preferential dissolution, but from precipitation of elementary suphur (see also Rimstidt and Vaughan, 2003). To resolve this issue, both surface and aqueous chemistry of iron and sulphur have to be taken into account to thoroughly interpret any experimental data on pyrite oxidation.

Few studies have focused on aqueous sulphur chemistry (Goldhaber, 1983; Steger and Desjardins, 1978; Schippers *et al.*, 1999 in the case of bioleaching), surely by a rising analytical difficulty. Unfortunately, ignoring aqueous chemistry does not allow using correct chemistry considerations for non stoichiometric dissolution processes. Basolo and Pearson (1958) concluded that any elementary redox reaction is certainly limited to a maximum of two electrons net transfer. Therefore, pyrite oxidation is expected to result in the production of several intermediate sulphoxyanions species of increasing oxidation numbers from (-I), as in FeS_2, to (+VI), as in SO_4^{2-}.

Williamson and Rimstidt (1994) have compiled data from different studies and hence proposed kinetic laws of pyrite oxidation in function of O_2, Fe(III) and both oxidants. They found that comparison between sulphur and iron contents from a study to another is very difficult since experimental configurations such as water/solid ratio, solid preparation, etc, greatly differed. To overcome this issue, Ichikuni (1960) focused on the ratio of total aqueous sulphur divided by total aqueous iron ($R = [S]_{tot}/[Fe]_{tot}$) to interpret his experimental data for the dissolution of pyrite in aqueous solutions at pH ranging from 1.1 to 3.2. A value of R = 2 corresponds to a stochiometric dissolution. Although parameter R can be used to directly compare dissolution experiments in different chemical and physical conditions, there is no other occurrence of this experimental parameter, to our knowledge. We decided to use similar treatment of experimental data, *i.e.* using the $R = [S]_{tot}/[Fe]_{tot}$ aqueous ratio measured in batch dissolution experiments at pH $\cong$ 2 in addition to solid characterization methods. Experiments were conducted in acidic media to avoid any iron hydrolysis and precipitation, with an initial pyrite surface free of any oxidation products and a monitoring of sulphur and iron aqueous speciations. With these controlled chemical conditions, we were able to verify experimentaly the hypothesis of Luther (1987 and 1997).

2. MATERIALS AND METHODS

2.1. Sample preparation

Centimetric cubic samples of pyrite from Spain (Logroño) were first dipped in 37% HCl during several hours to remove any oxidation products present at the mineral surface. The pyrite was then introduced in a glove box with partial pressures of H_2O ($p(H_2O)$) and O_2 ($p(O_2)$) both inferior to 1 vpm and rinsed with acetone. The mineral was ground in an agate mortar and sifted with ethanol (grain sizes in the 150 - 250 µm fraction). Pyrite was then washed in ultra-sonic bath to remove any fine particles adhering to the grain surface. These two operations were repeated until the ethanol after ultrasonic-bath was clear, and free of fine particles, as controlled by scanning electron microscopy (SEM). Samples were kept in a glove box for drying until experiments. Surface was controlled by X-ray photoelectron spectroscopy (XPS) showing no oxidation products. Chemical analysis was performed by SEM-based Electron x-ray dispersive spectroscopy over 40 points by sample and showed the stoichiometric ratio expected for pyrite (S/Fe = 1.99 ± 0.03). Moreover, sample characterization by X-ray diffraction (XRD) confirmed the absence of any accessory minerals, to the detection limit of XRD. The protocol of sample preparation has been controlled by other techniques, such as BET and dissolution experiments and is detailed elsewhere (Descostes, 2001 and Descostes *et al.*, 2002b). Additional solid characterization by XPS and nuclear microprobe are documented elsewhere (see Descostes *et al.*, 2000 and Descostes *et al.*, 2001).

2.3. Dissolution experiments

All solutions used in this study were made with ultrapure deionised water (18.2 MΩ cm^{-1}). Commercial salts and acid used are all of American Chemical Society (ACS) reagent grade or higher quality and purity. Experiments were run as batch experiments in glass electrochemistry cells used as reactors thermostated at 25.0 ± 0.1℃ in contact with atmospheric oxygen (20%). Agi tation was proceeded by a magnetic stirrer guaranteeing a solution continuously homogeneous. The water to solid ratio was of 150 $mL.g^{-1}$. Time course begun with pyrite introduction in solution. Dissolution experiments were carried out in acidic media HCl and $HClO_4$ around pH = 2 and 3 (Merck Titrisol #109970 and Prolabo Titrinorm #30111.291). Two different contact durations of ~ 6 h and ~ 24 h were selected to discriminate a hypothetical transient state from a stationary one. All experiments are detailed in table 1. Aliquots were sampled using first a pre-filter (Interchim #CH821770), then filtered at 0.22 µm (Nalgene #190-2520) and immediately analysed for sulphur and iron. The number of samples was limited to keep variations of the solid-solution ratio to < 10% of the initial value. The final solid samples were kept in anoxic glove box before XPS analysis.

2.3. Analysis

Sulphur aqueous speciation and analysis were performed by both ionic chromatography (Dionex analyser DX4500 using IonPac® AS14 analytical column and AG14 guard column in $[Na_2CO_3]$ = 3.5 mmol L^{-1} + $[NaHCO_3]$ = 1 mmol L^{-1} eluent) and capillary electrophoresis (Waters Quanta 4000), following protocols detailed in Motellier *et al.*, 1997 and Motellier and Descostes, 2000. $[Fe]_{tot}$ were determined by

furnace atomic absorption spectrometry (UNICAM 939, λ = 248.3 nm). Oxidation number of iron was investigated by spectrophotometry (Viollier *et al.*, 2000). Electrochemical parameters (pH and Eh) were followed after calibration (5 pH buffers and 1 Eh buffer) with a pH glass electrode (Radiometer #XG250) and a Pt electrode (Radiometer #XR110) each coupled with a calomel reference electrode (Radiometer #REF451) connected to an ionometer (Radiometer #PHM250). Data were collected and recorded on an informatic interface.

3. RESULTS AND INTERPRETATION

All results are gathered in tables 2 and 3. Only marginal variations of pH were observed during the dissolution duration, whatever the experiment considered. pH remaining quite constant can be easily understood, as the maximum amount of protons released upon dissolution (*i.e.*, $2 \times [Fe]_{tot}$ = 50 µmol L^{-1}) is negligible compared to $[H^+]_{init} \geq 10^{-3}$ M.

Eh initially dropped dramatically upon mineral introduction in the suspension, and then followed the same trend as a function of time as pH (figure 1). The initial decrease of Eh can be easily understood since Eh is not initially buffered by electroactive species, while the dissolution of pyrite will produce iron and sulphur, known for their electroactive behaviour. To check this interpretation, we compared Eh trends at about pH = 2, when adding an equivalent number of mole for pyrite, Fe(II) and Fe(0). The curves for pyrite and Fe(II) are superimposed, while Fe(0) addition induced less oxidative conditions (figure 2). Furthermore, calculations indicate that the Eh measured are consistent with Eh values imposed by Fe^{3+}/Fe^{2+} couple.

Trends of $[SO_4^{2-}]$ and $[Fe]_{tot}$ in function of time are different from a run to another for a same medium, indicating different dissolution rates (see figures 3 and 4). Let us consider $[HClO_4] = 10^{-2}$ mol L^{-1} medium for example: $[SO_4^{2-}]$ and $[Fe]_{tot}$ in runs M07, M10 and M22 are lower than in M04. At 360 minutes, $[Fe]_{tot}$ in runs M10 and M22 are respectively equal to 12 and 10 µmol L^{-1}, but is nearly twice higher (22 µmol L^{-1}) in M04 run. Dissolved Iron is mainly divalent (up to 95 % of $[Fe]_{tot}$) except for run M21 where Fe^{3+} predominates. Sulphur is exclusively under SO_4^{2-} form. No dissolved sulphoxyanion was detected. Furthermore, oxidation of samples by H_2O_2 did not show any difference between $[S]_{tot}$ and $[SO_4^{2-}]$. The great disparity in time in rates of $[SO_4^{2-}]$ and $[Fe]_{tot}$ increase can be traced to the presence of chemical impurities in pyrite. Indeed, Cruz *et al.* (2001) showed that others metallic sulphides in contact of pyrite induced a surface passivation, thereby strongly altering surface reactivity and so reducing the dissolution rate. Therefore, release rates are not convenient parameters to lay the foundations for a reactional mechanism of pyrite dissolution.

Whatever the variations of $[Fe_{aq}]$ and $[SO_4^{2-}]$, R ratios (= $[SO_4^{2-}]/[Fe]_{tot}$, as $[S]_{tot} = [SO_4^{2-}]$) eventually converge toward a value of R = 1.6, except for run M05 (figure 5). Furthermore, the dispersion in R values is smaller than in $[Fe]_{tot}$ and $[SO_4^{2-}]$. R seems therefore a more convenient experimental parameter. R varies in function of time, according to two distinct intervals. In the first interval, R > 2. This interval either can be very short, lasting less than 60 minutes in run M04, or can extend over the whole run duration, as for run M10 (figure 5). In this transient time interval R values are irreproducible from experiment to experiment. This period presumably corresponds to a first stage of pyrite dissolution. The second time interval is characterized by R values below 2, usually close to 1.60, but down to 1.25 for run

M21. Such R values are also observed for long duration experiment (see for example run M22, 1500 minutes) and may point to permanent dissolution regime. Only M05 experiment is out of comparison with R value close to 15 whatever run duration. We will only focus on the second time interval, because the R values are more reproducible and are assumed to be originated in a permanent dissolution state.

Through Eh conditions, iron is generally under Fe^{2+} or Fe^{3+} form and $[Fe]_{tot}$ values are below the solubility limits of all known ferric hydroxide or oxy-hydroxide minerals in the pH ranges of most of the experiments, except for the run M05. In the M05 case, R value close to 15, coupled with an increase of pH (pH = 3.00 to pH = 3.12) and low $[Fe]_{tot}$ (< 6 µmol L^{-1}, whereas $[SO_4^{2-}]$ increases up to 85 µmol L^{-1}) can be explained by precipitation of a ferric hydroxide compound. The short increase of pH is followed after 14 minutes by a decrease down to a pH value close to initial pH (figure 6). This variation squares with acidification produced by both pyrite dissolution and precipitation of ferric hydroxide or oxy-hydroxyde ($Fe(OH)_3$ or FeOOH) if iron produced by pyrite dissolution is estimated by the half of the sulphate content (*i.e.* 0.5 $\times$ 85 = 43 µmol L^{-1}).

4. DISCUSSION

4.1. Bibliographic comparison

Few data are available in literature. Most pyrite oxidation studies do not provide the values of measured concentration of iron and sulphur, or are even not interested in R ratio. Only Ichikuni (1960), McKibben and Barnes (1986) and Bonnissel-Gissinger *et al.* (1998) studies could be used to estimate R values. Data gathered in table 4 are extrapolated from kinetic curves published by these authors.

Ichikuni (1960) studied pyrite oxidation in [HCl] = 10^{-1} mol L^{-1} (pH = 1.89), [HCl] = 10^{-2} mol L^{-1} (pH = 2.0), [HCl] = 10^{-3} mol L^{-1} (pH = 2.9) and H_2O (pH = 3.2) in contact with atmosphere at 80°C. This author has calculated $[SO_4^{2-}]/[Fe]_{tot}$ from iron and sulphate production rates. We have recalculated ratios from $[SO_4^{2-}]$ and $[Fe]_{tot}$. Values diminish with the pH of the reactional medium, from R = 0.74 $\pm$ 0.02, to R = 1.38 $\pm$ 0.05, R = 1.92 $\pm$ 0.07 and R = 2.8 $\pm$ 0.1, for [HCl] = $10^{-1.5}$, 10^{-2}, 10^{-3} mol L^{-1} and H_2O media respectively. R > 2 measured in diluted medium (H_2O) reveals a deficit in aqueous iron, as in M05 experiment. Moderate pH tend to favour iron hydrolysis and precipitation as seen in Descostes *et al.*, (2002a). McKibben and Barnes (1986) studied pyrite oxidation in chlorhydric medium at pH = 1.89 in contact with atmosphere and H_2O_2 ($[H_2O_2]$ = 144 µmol L^{-1}) at 30°C. In these conditions R is always lower than 2, and the mean calculated R value equals 1.3 $\pm$ 0.1. Bonnissel-Gissinger *et al.* (1998) have carried out pyrite dissolution experiments in oxidizing conditions at several pH, notably at pH = 2.5 in HNO_3 medium at 25°C. The calculated R ratio for their experiments equals R = 1.6 $\pm$ 0.2 after 36 hours of dissolution.

When R ratios obtained in this study are compared to those from literature, three pH fields can be distinguished (figure 7). First, in very acidic to moderately acidic media (pH $\leq$ 2), R is inferior to 2. Results from our study are in good agreement with those from McKibben and Barnes (1986), Ichikuni (1960) and Bonnissel-Gissinger *et al.* (1998). We will discuss this point in the next section. Second, at pH = 3, R = 2 (maybe fortuitously) which is in agreement with the solid stoichiometry ratio of pyrite. Third, at pH > 3, R > 2, traducing iron precipitation by hydrolysis.

4.2. Reaction mechanism at pH < 3

Non stoichiometric dissolution with R < 2 can result either from an excess release of iron, leaving a sulphur-enriched layer at the pyrite surface, or from pyrite congruent dissolution followed by removal of dissolved sulphur species. The comparison of the different sets of experiments show that $[Fe]_{tot}$ are comparable for similar reaction periods, while $[SO_4^{2-}]$ can reach very low values in run M21 ([HCl] = $10^{-1.5}$ mol L^{-1}). In this last case, **R = 1.25** is the lowest value recorded for all experiments, likely indicating deficit in aqueous sulphur. Therefore, pyrite dissolution in acidic media is not congruent.

The only possible explanation for the observed non-stoichiometry in pyrite dissolution is that sulphur is removed from the solution, either as a solid, or as a gas; In both case, this removal indicates that sulphur species other than S_2^{2-} and SO_4^{2-}, the stable sulphur species, are present in the solution. Metastable sulphur species must form upon FeS_2 oxidation, and consequently the oxidation of pyrite into Fe^{2+} and SO_4^{2-} cannot be described by a single elementary step.

A logical explanation would merely trace $[SO_4^{2-}]$ deficit to the formation of a non soluble sulphur species (a gas or solid). This species could be one of the products of an intermediary disproportion (vérifie, je ne suis pas certain et recherche partout) step, while the other(s) product(s) of the disproportion would be soluble and further oxidized to S(VI). According to a thermodynamic approach, we have privileged the hypothesis of a disproportion of a sulphur specie in acidic medium with an oxidation number lying between S^0 and SO_4^{2-}. First, pyrite dissolves, with release of an aqueous sulphur species $S^{(n)}$ ($0 < n < 6$) according to

$$FeS_2 \rightarrow Fe^{2+} + 2\ S^{(n)} + 2\ (n+1)\ e^- . \qquad (5)$$

$S^{(n)}$ specie should then disproportionate into another sulphur specie $S^{(n')}$ with an oxidation number n' ($n' > n$), and metastable S^0 (which would not be oxidized for thermodynamic or kinetic reasons) according to the reaction:

$$S^{(n)} \rightarrow \frac{n}{n'} S^{(n')} + \frac{n'-n}{n'} S^0 \qquad (6)$$

Finally, $S^{(n')}$ specie would be oxidized into SO_4^{2-} in a third stage:

$$S^{(n')} \rightarrow S^{(VI)} + (6 - n')\ e^- \qquad (7)$$

Mass balance for Reaction (7) is

$$[SO_4^{2-}] = [S^{(VI)}] = [S^{(n')}] \qquad (8)$$

Mass balance for Reaction (6) is

$$\left[S^{(n)}\right] = \frac{n'}{n}\left[S^{(n')}\right] = \frac{n'}{n}\left[SO_4^{2-}\right], \qquad (9)$$

where Equation (8) was reported into the right member of Equation 9. Mass balance for Reaction (5) is

$$\left[\mathrm{Fe}\right]_{\mathrm{total}} = \left[\mathrm{Fe}^{2+}\right] = 0.5\ \left[\mathrm{S}^{(\mathrm{n})}\right] = 0.5\,\frac{\mathrm{n}'}{\mathrm{n}}\left[\mathrm{SO}_4^{2-}\right] \qquad (10)$$

where Equation (9) was reported in the right member of Equation (10). Finally from Equation (10), $R = [SO_4^{2-}]/[Fe]_{tot}$ can be easily expressed as

$$\mathrm{R} = \frac{2\mathrm{n}}{\mathrm{n}'} \qquad (11)$$

With $0 < n < n' \leq 6$. The net oxidation reaction is obtained by reporting reactions (6) and (7) into reaction (5), consistent with equation (11):

$$\mathrm{FeS_2} \rightarrow \mathrm{Fe}^{2+} + 2\left[1 + \frac{6\,\mathrm{n}}{\mathrm{n}'}\right]\mathrm{e}^{-} + \frac{2\mathrm{n}}{\mathrm{n}'}\,\mathrm{S}^{\mathrm{VI}} + 2\,\frac{\mathrm{n}'-\mathrm{n}}{\mathrm{n}'}\,\mathrm{S}^{0} \qquad (12)$$

Notations $S^{(n)}$ refer to species $S_xO_y^{z-}$, where $n = (-z + 2y)/x$. The overall pyrite oxidation reaction can be written as (Descostes, 2001)

$$\mathrm{FeS_2} + \frac{6\mathrm{n}+\mathrm{n}'}{2\mathrm{n}'}\,\mathrm{O_2} + \frac{2\mathrm{n}-\mathrm{n}'}{\mathrm{n}'}\,\mathrm{H_2O} \rightarrow \mathrm{Fe}^{2+} + \frac{2\mathrm{n}}{\mathrm{n}'}\,\mathrm{SO}_4^{2-} + \frac{2(\mathrm{n}'-\mathrm{n})}{\mathrm{n}'}\,\mathrm{S}^{0} + 2\left(\frac{2\mathrm{n}-\mathrm{n}'}{\mathrm{n}'}\right)\mathrm{H}^{+} \qquad (13)$$

Table 5 collects values of $R \leq 2$ for different possible values of *n* and *n'*, where disproportion reactions are thermodynamically possible for different known sulphur species $S^{(n)}$ and $S^{(n')}$. Several ($S^{(n)}$, $S^{(n')}$) couples can theoretically generate $R \leq 2$. Among them, the ($S_2O_3^{2-}$; $S_4O_6^{2-}$) couple is plausible for several reasons discussed below. It corresponds to $R = 2 \times 2/2.5 = 1.6$.

4.3. Disproportion of thiosulfate

Several couples ($S^{(n)}$, $S^{(n')}$) can theoretically generate a $[SO_4^{2-}]/[Fe]_{tot}$ ratio inferior to 2. Among them, the ($S_2O_3^{2-}$; $S_4O_6^{2-}$) couple is plausible for the following reasons:

(1) Thiosulphate has already been detected in such dissolution experiments in carbonated media (see Descostes *et al.*, 2002a);
(2) Thiosulphate has a mean number of oxidation equal to 2 and is thought to be the first aqueous sulphur specie released from pyrite surface (see Luther, 1987; Descostes *et al.*, 2001; Rimstidt and Vaughan, 2003);
(3) Thiosulphate oxidation into tetrathionate is possible in only one elementary reaction since the number of transferred electrons is inferior to 2 (Basolo and Pearson, 1958);
(4) Thiosulfate and tetrathionate are expected to be metastable before the formation of sulphate ions in our experimental conditions (figure 8);
(5) The observed variation of R as a function of pH can be explained by the stability domains of pyrite, thiosulphate, elementary sulphur and tetrathionate (figure 8). Thiosulphate ion is unstable in acidic medium from pH = 3. It

disproportionates into S^0 and $S_4O_6^{2-}$. Tetrathionate ion would then be rapidly oxidized into sulphate. As pH decreases, the proportion of S^0 increases. $[SO_4^{2-}]/[Fe]_{tot}$ ratio then decreases. However, as we will discuss below, this trend can as well be assigned to the exsolution of SO_2.

The proposed pyrite oxidation in acidic medium can be synthesized by the following reactional sequence (corresponding ΔG_R are indicated) with a first step without acidification:

$$FeS_2 + 3/2\ O_2(g) \rightarrow Fe^{2+} + S_2O_3^{2-} \quad (14)$$

quand tu donnes ΔG_R, il faut préciser (g) (aq) etc au moins à chaque fois qu'il y a ambiguïté (recherche partout)

$\Delta G_R = -445.9$ kJ mol^{-1}

$$S_2O_3^{2-} + 6/5\ H^+ \rightarrow 2/5\ S^0 + 2/5\ S_4O_6^{2-} + 3/5\ H_2O \quad (15)$$

$\Delta G_R = -36.0$ kJ mol^{-1}

$$S_4O_6^{2-} + 7/2\ O_2 + 3\ H_2O \rightarrow 4\ SO_4^{2-} + 6\ H^+ \quad (16)$$

$\Delta G_R = -1224.0$ kJ.mol^{-1}

This latter reaction can tentatively be divided in to two other intermediary steps with the production of sulphite (SO_3^{2-}) in order to respect the rule of the limited electron number transferred and its observation in alkaline media (Descostes *et al.*, 2002a) according to:

$$S_4O_6^{2-} + 3/2\ O_2 + 3\ H_2O \rightarrow 4\ SO_3^{2-} + 6\ H^+ \quad (17)$$

$\Delta G_R = -193.5$ kJ mol^{-1}

and

$$SO_3^{2-} + 1/2\ O_2 \rightarrow SO_4^{2-} \quad (18)$$

$\Delta G_R = -257.6$ kJ mol^{-1}

Hence, the overall reaction (*i.e.* reaction 13 when R = 1.6) is

$$FeS_2 + 2.9\ O_2 + 0.6\ H_2O \rightarrow Fe^{2+} + 0.4\ S^0 + 1.6\ SO_4^{2-} + 1.2\ H^+ . \quad (19)$$

$\Delta G_R = -971{,}5$ kJ mol^{-1}

In more acidic conditions, SO_2 formation has to be taken into account according to the corresponding overall reaction:

$$FeS_2 + 2.1\ O_2 + 2\ H^+ \rightarrow Fe^{2+} + 0.4\ S^0 + 1.6\ SO_{2(g)} + H_2O \quad (20)$$

S^0 precipitation, as a consequence of thiosulphate disproportion is enough to explain the sulphur deficit observed in solution (figure 7). However experimental R values are not absolutely equal to R = 1.6. Reaction (12) might not be complete or another step of disproportion should be considered from notably $S_3O_6^{2-}$ as proposed by Schippers *et al.* (1999) or sulphite (SO_3^{2-}). In the first case, a ratio equal to 1.20 is expected. A similar value is found when the first released sulphoxyanion considered is $S_5O_6^{2-}$. We prefer to assign ratios inferior to 1.6 to sulphite. Thiosulphate, as we discussed before, is thought to be the first aqueous sulphur specie released during the pyrite oxidation mechanism. Moreover, SO_3^{2-} in acidic conditions is stable under SO_2 form (figure 8). If thiosulphate is the first aqueous species R = 1.00. Hence, our

experimental observations can be explained by a partial exsolution of SO_2in that case, which would tend to increase the aqueous sulphur deficit, leading to R values between 1.6 and 1.00, depending on pH.

However, our observations could not fully validate this reactional model. Thiosulphate and tetrathionate ions have not been detected. Kinetic oxidation into sulphate in acidic medium would be in this case too fast. Taylor *et al.* (1984) proposed similar conclusions by observing no sulphur isotopic fractioning between sulphate ions and pyrite during its oxidation in oxygenated conditions. They interpret this result by the absence of any intermediary sulphoxyanion during pyrite oxidation, or by a very short lifetime.

Moreover, we have not detected any precipitation of S^0 by either XPS, nuclear microprobe or observation of filtrates by SEM. We can put forward the small amounts of mater involved. In the case of M21 experiment, the total amount of S^0 was $1.8.10^{-6}$ mol L^{-1} at the end of the run, that is to say 32 ppm while XPS detection limit is 1000 ppm. We can also invoke the instability of elementary sulphur under vacuum conditions: it is volatile and tends to sublimate from 270 K under vacuum conditions (Mycroft *et al.*, 1990).

Nevertheless, the disproportion of thiosulphate ions into S^0 and $S_4O_6^{2-}$ is consistent with thermodynamic considerations (Charlot, 1959; figure 8) and mechanisms proposed by Luther (1997), Kelsall *et al.* (1999) and Rimstidt and Vaughan (2003). It is therefore not needed to assume iron preferential dissolution in acidic media (Ahlberg and Broo, 1997; Buckley and Woods, 1987; Mycroft *et al.*, 1990; Sasaki *et al.,* 1995; Zhu *et al.,* 1994). Sulphur deficit in acidic media has also been observed for dissolution experiment of durations longer than 24 hours (experiment M22, R = 1.3).

4.4. Comparison with others models

Sulphur deficit at pH<3 cannot reasonably be originated in precipitation of any known ferric or ferrous salt, since in these conditions the saturation indices are lower than 1.

Sulphur can precipitate under S^0 form. According to this hypothesis, we have verified that sulphur deficit was not associated with equilibrium conditions of the system FeS_2 / S^0 / SO_4^{2-}. We calculated that measured Eh and pH values do not actually correspond to the precipitation of S^0 (see Descostes, 2001 for more details). Besides, if experimental Eh measurements were not significant for kinetic reasons, Eh can be calculated assuming equilibrium conditions were achieved for the species FeS_2 / S^0 / SO_4^{2-}:

$$\frac{3}{7}FeS_2 + \frac{1}{7}1/3\ SO_4^{2-} + \frac{8}{7}H^+ \Leftrightarrow \frac{3}{7}Fe^{2+} + S^0 + \frac{4}{7}H_2O \qquad (21)$$

$$K^{-7} = \frac{[SO_4^{2-}]\,[H^+]^8}{[Fe^{2+}]^3}$$

where lg K = -1.1, rearranging

$\lg \frac{[Fe^{2+}]}{[SO_4^{2-}]^{1/3}}$ = 2.6 -(-lg[H^+]) which does not correspond to our experimental observations.

We have already seen that ferric iron can be reduced by pyrite in acidic medium (Singer and Stumm, 1970) according to the reaction

$$FeS_2 + 14\ Fe^{3+} + 8\ H_2O \rightarrow 15\ Fe^{2+} + 2\ SO_4^{2-} + 16\ H^+ \ . \qquad (3)$$

This hypothesis is not verified since R would be equal to 0.133 in that case.

Sulphur from pyrite can disproportionate into SO_4^{2-} and H_2S or with production of pyrrhotite ($Fe_{0.887}S$) according to reactions

$$FeS_2 + 3/2\ O_2 + H_2O \rightarrow Fe^{2+} + H_2S + SO_4^{2-} \qquad (22)$$
($\Delta G°_R$ = -458.3 kJ mol^{-1})
and
$$FeS_2 + 1.5565\ O_2 + 0.887\ H_2O \rightarrow Fe_{0.887}S + SO_4^{2-} + 0.113\ Fe^{2+} + 1.774\ H^+ \qquad (23)$$
($\Delta G°_R$ = -483.7 kJ mol^{-1}).

These two reactions are both thermodynamically possible. In the first case, H_2S should tend in acidic medium to transform into $H_2S_{(gas)}$ and disappear by outgazing towards atmosphere, generating an aqueous sulphur deficit. However, the $[SO_4^{2-}]/[Fe]_{tot}$ ratio is fixed by the number of transferred electrons during the reaction (see Equ.11). It is in this case equal to R = 1, which was not observed in our study. In the second case R = 8.8 is expected. It might correspond to the first stages of pyrite dissolution where calculated ratios were superior to R = 2. Nevertheless, saturation indexes are inferior to 1, invalidating therefore this hypothesis.
Our approach fits the formalism developed by Bailey and Peters (1976). These authors proposed that pyrite oxidation into sulphate is accompanied by precipitation of S^0:

$$FeS_2 + (½+3/2y+¼x)O_2 + (2+x-2y)H^+ \leftrightarrow (1-x)Fe^{2+} + xFe^{3+} + (2-y)S^0 + ySO_4^{2-} + (1-y-½x)H_2O \qquad (24)$$

We have modelled experiments carried out at pH ≅ 2 and pH ≅ 1.5. The corresponding equilibria would be:

$$FeS_2 + 2.7875\ O_2 + 0.425\ H_2O \leftrightarrow 0.85\ Fe^{2+} + 0.15\ Fe^{3+} + 0.5\ S^0 + 1.5\ SO_4^{2-} + 0.85\ H^+ \qquad (25)$$
$$FeS_2 + 2.6075\ O_2 + 0.43\ H^+ \leftrightarrow 0.07\ Fe^{2+} + 0.93\ Fe^{3+} + 0.75\ S^0 + 1.25SO_4^{2-} + 0.215H_2O \qquad (26)$$

For these chemical reactions, the $\Delta G°_R$ values are negative (-927.5 and -838.5 kJ.mol^{-1} respectively). However COMMENT LE SAIS-TU ? it is only a balance (and not a mechanism) with two degrees of freedom: x and y corresponding respectively to the progress of iron and sulphur oxidation.

Finally, the last published study from McGuirre *et al.* (2001) also shows the presence of elementary sulphur on an oxidized pyrite surface in acidic medium (pH = 1 in sulphuric medium and in presence of 500 ppm of Fe^{3+}, duration = 96 h, T = 42°C). These authors have underlined by Raman micro scopy a heterogeneous distribution of oxidation products at the pyrite surface, as observed also by nuclear microprobe (Descostes *et al.*, 2001).

5. CONCLUSION

Mechanisms of pyrite oxidation in acidic medium were investigated by batch experiments at 25.0℃ in contact with atmosphere at pH around 2, and by reconsideration of previously published data. A particular effort was made to prepare a pristine pyrite surface without any oxidation products thanks to the use of anoxic atmosphere. Using the R parameter $R = [S]_{tot}/[Fe]_{tot}$ was central to understanding the evolution of the dissolution stoichiometry as a function of pH. R values below the S/Fe stoichiometric ratio in pyrite (*i.e.*, S/Fe = 2) can be traced to an aqueous deficit in sulphur according to multi-step mechanisms.

The first step sees the production of a thiosulfate. This specie would disproportionate into tetrathionate and another S specie that would disappear from solution, since it is a solid compound (typically S^0). Tetrathionate would finally be oxidized into sulphate. Experimental $R = [SO_4^{2-}]/[Fe]_{tot} = 1.60$ can then be smartly predicted and is equal to the double of the ratio of the numbers of oxidation of each intermediate sulphoxyanion considered. In more acidic conditions, SO_2 formation followed by an exsolution is consistent with lower experimental values for R (R = 1.25).

These mechanisms, according to a simple thermodynamic approach, are in fair agreement with most experimental published data. $S_2O_3^{2-}$ disproportion is enough to explain the observed aqueous sulphur deficit. It is therefore not needed to assume iron preferential dissolution in acidic media usually accepted and proposed in the literature (Ahlberg and Broo, 1997; Buckley and Woods, 1987; Mycroft *et al.*, 1990; Sasaki *et al.,* 1995; Zhu *et al.,* 1994). We propose rather the disproportion of aqueous sulphur which results in a non congruent dissolution of pyrite.

However, further experiments are needed to confirm this mechanism, especially to identify the presence of S^0. One should take into account, initial surface pyrite without any oxidation products and promote the combination of aqueous chemistry and solid characterisation.

This experimental approach should be applied to most sulphide mineral, in particular to pyrrhotite ($Fe_{1-x}S$) which is known to dissolve with production of $H_2S_{(g)}$. In this latter case, disproportion and exsolution reactions should complicate the reactional mechanism.

ACKNOWLEDGMENTS

The support of the “Agence Nationale pour la gestion des Déchets Radioactifs” through grant FT00-1-066 is gratefully acknowledged. We thank Michel Schlegel of CEA for insightful comments.

REFERENCES

Ahlberg E. and Broo A.E. (1997) Electrochemical reaction mechanisms at pyrite in acidic perchlorate solutions. *Journal - Electrochemical Society* **144**, 1281-1285.

Bailey L.K. and Peters E. (1976) Decomposition of pyrite in acids by pressure leaching and anodization: The case for an electrochemical mechanism. *Canadian Metallurgical Quarterly* **15**, 333-344.

Basolo F. and Pearson R.G. (1958) *Mechanisms of inorganic reactions: A study of metals complexes in solution*. Wiley, New York.

Beaucaire C., Pitsch H., Toulhoat P., Motellier S. and Louvat D. (2000) Regional fluid characterisation and modelling of water-rock equilibria in the Boom clay Formation and in the Rupelian aquifer at Mol, Belgium. *Applied Geochemistry* **15**, 667-686.

Berner R.A. (1984) Sedimentary pyrite formation: An update. *Geochimica et Cosmochimica Acta* **48**, 605-615.

Biegler T. and Swift D.A. (1979) Anodic behavior of pyrite in acid solutions. *Electrochimica Acta* **24**, 415-420.

Bonnissel-Gissinger P., Alnot M., Ehrhardt J.-J. and Behra P. (1998) Surface oxidation of Pyrite as a function of pH. *Environmental Science and Technology* **32**, 2839-2845.

Buckley A.N. and Woods R. (1987) The surface oxidation of pyrite. *Applied Surface Science* **27**, 437-452.

Charlot G., Badoz-Lambling J. and Trémillon B. (1959) *Les réactions électrochimiques. Méthodes électrochimiques d'analyse.* Editions Masson & Cie, Paris.

Cruz R., Bertrand V., Monroy M. and Gonzalez I. (2001) Effect of sulfide impurities on the reactivity of pyrite and pyritic concentrates: a multi-tool approach. *Applied Geochemistry* **16**, 803-819.

Descostes M. (2001) Evaluation d'une perturbation oxydante en milieu argileux : mécanismes d'oxydation de la pyrite (FeS_2). Ph. D. Thesis, Université Denis Diderot Paris VII.

Descostes M., Mercier F., Thromat N., Beaucaire C. and Gautier-Soyer M. (2000) Use of XPS to the determination of chemical environment and oxidation state of iron and sulfur samples: Constitution of a data basis in binding energies for Fe and S reference compounds and applications to the evidence of surface species of an oxidized pyrite in a carbonate medium. *Applied Surface Science* **165**, 288-302.

Descostes M., Mercier F., Beaucaire C., Zuddas P., and Trocellier P. (2001) Nature and distribution of chemical species on oxidized pyrite surface: complementarity of XPS and Nuclear Microprobe Analysis. *Nuclear Inst. and Methods in Phys. Research B* **181**, 603-609.

Descostes M., Beaucaire C., Mercier F., Savoye S., Sow J. and Zuddas P. (2002a) Effect of carbonate ions on pyrite (FeS_2) dissolution. *Bull. Soc. géol. France* **173**, 265-270.

Descostes M., Mercier F., Bassot S. and Beaucaire C. (2002b) *in preparation*.

Donato P., Mustin C., Benoit R. and Erre R. (1993) Spatial distribution of iron and sulfur species on the surface of pyrite. *Applied Surface Science* **68**, 81-93.

Ennaoui A., Fiechter S., Jaegermann W. and Tributsch H. (1986) Photoelectrochemistry of highly quantum efficient single-crystalline n-FeS_2 (pyrite). *Journal Electrochemical Society* **133**, 97-106.

Evangelou V.P.B. (1995) *Pyrite oxidation and its control*. CRC Press.

Fornasiero D., Eijt V. and Ralston J. (1992) An electrokinetic study of pyrite oxidation. *Colloids and Surfaces* **62**, 63-73.

Garrels R.M. and Thomson M.E. (1960) Oxidation of pyrite by iron sulfate solutions. *American Journal of Science* **258-A**, 57-67.

Goldhaber M.B. (1983) Experimental study of metastable sulfur oxyanion formation during pyrite oxidation at pH 6-9 and 30°C. *American Journal of Science* **238**, 193-217.

Guevremont J.M., Elsetinow A.R., Strongin D.R., Bebie J. and Schoonen M.A.A. (1998) Structure sensitivity of pyrite oxidation: comparison of the (100) and (111) planes. *American Mineralogist* **83**, 1353-1356.

Ichikuni P.M. (1960) Sur la dissolution des minerais sulfurés en divers milieux. *Bull. Chem. Soc. Japan* **33**, 1052-1057.

Kamei G. and Ohmoto H. (2000) The kinetics of reactions between pyrite and O_2-bearing water revealed from in situ monitoring DO, Eh and pH in a closed system. *Geochimica et Cosmochimica Acta* **64**, 2585-2601.

Kelsall G.H., Yin Q., Vaughan D.J., England K.E.R. and Brandon N.P. (1999) Electrochemical oxidation of pyrite (FeS_2) in aqueous electrolytes. *Journal of Electroanalytical Chemistry* **471**, 116-125.

Knipe S.W., Mycroft J.R., Pratt A.R., Nesbitt H.W. and Bancroft G.M. (1995) X-ray photoelectron spectroscopy study of water adsorption on iron sulphide minerals. *Geochimica et Cosmochimica Acta* **59**, 1079-1090.

Luther III G.W. (1987) Pyrite oxidation and reduction: Molecular orbital theory considerations. *Geochimica et Cosmochimica Acta* **51**, 3193-3199.

Luther III G.W. (1997) Comment on "Confirmation of a sulfur-rich layer on pyrite after oxidative dissolution by Fe(III) ions around pH 2" by Sasaki K., Tsunekawa M., Tanaka S. et Konno H. *Geochimica et Cosmochimica Acta* **61**, 3269-3271.

McClendon J. H. (1999) The origin of life. *Earth-Science Reviews* **47**, 71-93.

McGuirre M.M., Jallad K.N., Ben-Amotz D. and Hamers R.J. (2001) Chemical mapping of elemental sulfur on pyrite and arsenopyrite surfaces using near-infrared Raman imaging microscopy. *Applied Surface Science* **178**, 105-115.

McKibben M.A. and Barnes H.L. (1986) Oxidation of pyrite in low temperature acidic solutions: rate laws and surface textures. *Geochimica et Cosmochimica Acta* **50**, 1509-1520.

Moses C.O., Nordstrom D.K., Herman J.S. and Mills A.L. (1987) Aqueous pyrite oxidation by dissolved oxygen and ferric iron. *Geochimica et Cosmochimica Acta* **51**, 1561-1571.

Motellier S., Gurdale K. and Pitsch H. (1997) Sulfur speciation by capillary electrophosis with indirect spectrophotometric detection: in search of a suitable carrier electrolyte to maximize sensitivity. *Journal of Chromatography A* **770**, 311-319.

Motellier S. and Descostes M. (2001) Sulfur speciation and tetrathionate sulfitolysis monitoring by capillary electrophosis. *Journal of Chromatography A* **907**, 329-335.

Mycroft J.R., Mcintyre N.S., Lorimer J.W. and Hill I.R. (1990) Detection of sulfur and polysulphides on electrochemically oxidized pyrite surfaces by X-ray photoelectron spectroscopy and Raman spectroscopy. *J. Electranal. Chem.* **292**, 139-152.

Nesbitt H.W., Scaini M.J., Höchst H., Bancroft G.M., Schaufuss A.G. and Szargan R. (2000) Synchrotron XPS evidence for Fe^{2+}-S and Fe^{3+}-S surface species on pyrite fracture-surfaces, and their 3D electonic states. *American Mineralogist* **85**, 850-857.

Nicholson R.V., Gillham R.W. and Reardon E.J. (1988) Pyrite oxidation in carbonate-buffered solution: 1. Experimental kinetics. *Geochimica et Cosmochimica Acta* **52**, 1077-1085.

Nicholson R.V., Gillham R.W. and Reardon E.J. (1990) Pyrite oxidation in carbonate-buffered solution: 2. Rate control by oxide coatings. *Geochimica et Cosmochimica Acta* **54**, 395-402.

Pain D.J., Sanchez A. and Meharg A.A. (1998) The Doñana ecological disaster: contamination of a world heritage estuarine marsh ecosystem with acidified pyrite mine waste. *The Science Of The Total Environment* **222**, 45-54.

Rich R.A., Holland H.D. and Petersen U. (1977) Hydrothermal uranium deposits. In *Developments in Economic Geology* **6**, Elsevier.

Rimstidt J.D. and Vaughan D.J. (2003) Pyrite oxidation: A state-of-the-art assessment of the reaction mechanism. *Geochimica et Cosmochimica Acta* **67**, 873-880.

Rosso K.M., Becker U. and Hochella M.F. Jr. (1999a) Atomically resolved electronic structure of pyrite {100} surfaces: An experimental and theoretical investigation with implications for reactivity. *American Mineralogist* **84**, 1535-1548.

Rosso K.M., Becker U. and Hochella M.F. Jr. (1999b) The interaction of pyrite {100} surfaces with O_2 and H_2O: Fundamental oxidation mechanisms. *American Mineralogist* **84**, 1549-1561.

Sasaki K., Tsunekawa M., Tanaka S. and Konno H. (1995) Confirmation of a sulfur-rich layer on pyrite after oxidative dissolution by Fe(III) ions around pH 2. *Geochimica et Cosmochimica Acta* **59**, 3155-3158.

Sasaki K., Tsunekawa M., Tanaka S. and Konno H. (1997) Reply to the comment by G. W. Luther III on "Confirmation of a sulfur-rich layer on pyrite after oxidative dissolution by Fe(III) ions around pH 2". *Geochimica et Cosmochimica Acta* **61**, 3273-3274.

Scaini M.J., Bancroft G.M. and Knipe S.W. (1997) An XPS, AES, and SEM study of the interactions of gold and silver chloride species with PbS and FeS_2: Comparison to natural samples. *Geochimica et Cosmochimica Acta* **61**, 1223-1231.

Schaufuss A.G., Nesbitt H.W., Kartio I., Laajalehto K., Bancroft G.M. and Szargan R. (1998) Reactivity of surface chemical states on fractured pyrite. *Surface Science* **411**, 321-328.

Schippers A., Rohwerder T. and Sand W. (1999) Intermediary sulfur compounds in pyrite oxidation: implications for bioleaching and biodepyritization of coal. *Appl. Microbiol. Biotechnol.* **52**, 104-110.

Singer P.C. and Stumm W. (1970) Acid mine drainage: The rate-limiting step. *Science* **167**, 1121-1123.

Steger H.F. and Desjardins L.E. (1978) Oxidation of sulfide minerals, 4. Pyrite, chalcopyrite and pyrrhotite. *Chemical Geology* **23**, 225-237.

Taylor B.E., Wheeler M.C. and Nordstrom D.K. (1984) Stable isotope geochemistry of acid mine drainage: Experimental oxidation of pyrite. *Geochimica et Cosmochimica Acta* **48**, 2669-2678.

Toniazzo V., Mustin C., Portal J.M., Humbert B. and Erre R. (1999) Elemental sulfur at the pyrite surfaces: speciation and quantification. *Applied Surface Science* **143**, 229-237.

Uhlig I., Szargan R., Nesbitt H.W. and Laajalehto K. (2001) Surface states and reactivity of pyrite and marcasite. *Applied Surface Science* **179**, 222-229.

Viollier E., Inglett P.W., Hunter K., Roychoudhury A.N. and Van Cappellen P. (2000) The ferrozine method revisited: Fe(II)/Fe(III) determination in natural waters. *Applied Geochemistry* **15**, 785-790.

Wächtershäuser G. (2000) Life as we don't know it. *Science* **289**, 1307-1308.

Wei D. and Osseo-Asare K. (1997) Semiconductor electrochemistry of particulate pyrite mechanisms and products of dissolution. *Journal Electrochemical Society* **144**, 546-553.

Williamson M.A. and Rimstidt J.D. (1994) The kinetics and electrochemical rate-determining step of aqueous pyrite oxydation. *Geochimica et Cosmochimica Acta* **58**, 5443-5454.

Zhu X., Li J. and Wadsworth M.E. (1994) Characterization of surface layers formed during pyrite oxidation. *Colloids and Surface A: Physicochemical and Engineering Aspects* **93**, 201-210.

TABLE AND FIGURE CAPTIONS

Table 1: Details of each dissolution experiment.
Table 2: Analytical results for runs in $[HClO_4] = 10^{-2}$ mol L^{-1} medium.
Table 3: Analytical results for runs in $[HCl] = 10^{-1.5}$ and 10^{-2} mol L^{-1} and $[HClO_4] = 10^{-3}$ mol L^{-1} media.
Table 4: Ratios $R = [SO_4^{2-}]/[Fe]_{tot}$ calculated from data taken from Ichikuni (1960), McKibben and Barnes (1986) and Bonnissel-Gissinger *et al.* (1998).
Table 5: Ratios $[SO_4^{2-}]/[Fe]_{tot}$ (R) inferior or equal to 2 in function of $S^{(n)}$ and $S^{(n')}$ ($0 < n < n'$ and $n' \leq 6$) inherited from the pyrite oxidation with a disproportion step into S^0; ΔG_R of the disproportion step is also indicated (in kJ mol^{-1}). See Descostes (2001) for thermodynamic data.

Figure 1: Comparison of redox potential (Eh) trends in $[HCl] = 10^{-2}$ mol L^{-1} (run M13) and $[HCl] = 10^{-1.5}$ mol L^{-1} (run M21) media.
Figure 2: Eh trends in $[HCl] = 10^{-2}$ mol L^{-1} medium for different iron oxidation number.
Figure 3: Comparison of sulphate contents trends (**A**: $[HClO_4] = 10^{-2}$ mol L^{-1} – runs M04, M07, M10 and M22; **B**: $[HCl] = 10^{-1.5}$ mol L^{-1} – run M21, $[HCl] = 10^{-2}$ mol L^{-1} – run M13 $[HClO_4] = 10^{-3}$ mol L^{-1} – runs M05 and M19).
Figure 4: Comparison of iron contents trends (**A**: $[HClO_4] = 10^{-2}$ mol L^{-1} – runs M04, M07, M10 and M22; **B**: $[HCl] = 10^{-1.5}$ mol L^{-1} – run M21, $[HCl] = 10^{-2}$ mol L^{-1} – run M13 $[HClO_4] = 10^{-3}$ mol L^{-1} – runs M05 and M19).
Figure 5: Comparison of ratios $R = [SO_4^{2-}]/[Fe]_{tot}$ trends (**A**: $[HClO_4] = 10^{-2}$ mol L^{-1} – runs M04, M07, M10 and M22; **B**: $[HCl] = 10^{-1.5}$ mol L^{-1} – run M21, $[HCl] = 10^{-2}$ mol L^{-1} – run M13 $[HClO_4] = 10^{-3}$ mol L^{-1} – runs M05 and M19).
Figure 6: Comparison of pH trends in $[HClO_4] = 10^{-3}$ mol L^{-1} medium (runs M05 and M19).
Figure 7: Comparison of ratios $R = [SO_4^{2-}]/[Fe]_{tot}$ calculated in this study and from data taken from literature.
Figure 8: Eh-pH diagram for sulphur - iron - water system at 25°C, considering only sulphur species with an oxidation number inferior to sulphate ($[\Sigma S] = 2 \times [\Sigma Fe] = 2.10^{-5}$ mol L^{-1}). See Descostes (2001) for thermodynamic data.

TABLES

Table 1: Details of each dissolution experiment.

Run	Media	Duration (min)
M02	$HClO_4$ 10^{-2} mol L^{-1}	294
M04	$HClO_4$ 10^{-2} mol L^{-1}	369
M05	$HClO_4$ 10^{-3} mol L^{-1}	471
M07	$HClO_4$ 10^{-2} mol L^{-1}	261
M10	$HClO_4$ 10^{-2} mol L^{-1}	361
M12	$HClO_4$ 10^{-2} mol L^{-1}	406
M13	HCl 10^{-2} mol L^{-1}	365
M19	$HClO_4$ 10^{-3} mol L^{-1}	360
M21	HCl $10^{-1.5}$ mol L^{-1}	360
M22	$HClO_4$ 10^{-2} mol L^{-1}	1507

Table 2: Analytical results for runs in [$HClO_4$] = 10^{-2} mol L^{-1} medium.

Run	Medium	Time	[Fe]	σ	$Fe^{(II)}$	σ	$Fe^{(III)}$	σ	[SO_4^{2-}]	σ	R	σ	pH	Eh
		min	*µmol L^{-1}*		*%*				*µmol L^{-1}*					*MV/ESH*
M04	[$HClO_4$] = 10^{-2} mol L^{-1}	0	0	0	--	--	--	--	0	0	--	--	2.089	732.5
		5	6.5	0.7	79.7	4.0	20.3	1.0	12	1	1.8	0.3	2.092	667.2
		21	9.9	0.7	72	4	28	1	18	1	1.8	0.2	2.107	667.5
		33	12.6	0.7	94	5	6.2	0.3	19	2	1.5	0.2	2.114	662.8
		43	16.6	0.8	89	4	10.8	0.5	16	1	0.96	0.08	2.116	664.8
		66	17.5	0.8	85	4	14.9	0.7	20.5	0.8	1.171	0.070	2.121	665.2
		128	19.3	0.8	93	5	7.1	0.4	24	3	1.2	0.2	2.114	668.5
		166	15.3	0.8	78	4	21.7	1.1	22	1	1.438	0.100	2.114	670.3
		216	20.4	0.7	98	5	2.1	0.1	28	1	1.37	0.07	2.102	672.8
		281	21.0	1.0	80.5	4.0	19.5	1.0	31	3	1.5	0.2	2.107	675.2
		369	22.0	0.9	89	4	11.5	0.6	94	2	4.27	0.20	2.099	--
M07	[$HClO_4$] = 10^{-2} mol L^{-1}	0	0	0	--	--	--	--	0	0	--	--	2.032	762.5
		5	2.3	0.3	--	--	--	--	3.5	0.3	1.5	0.3	2.042	705
		25	4.3	0.6	--	--	--	--	5.7	0.4	1.3	0.2	2.057	691.1
		46.5	4.2	0.6	--	--	--	--	6.5	0.3	1.5	0.2	2.05	685.5
		93	4.5	0.7	--	--	--	--	8.2	0.3	1.8	0.3	2.045	671.1
		189	5.8	0.9	--	--	--	--	9.0	0.4	1.5	0.2	2.049	655.3
		261	6.4	1.0	--	--	--	--	9.0	0.4	1.4	0.2	2.050	644.9
M10	[$HClO_4$] = 10^{-2} mol L^{-1}	0	0	0	--	--	--	--	0	0	--	--	2.041	726.0
		5	2.1	0.3	79	4	22	1	5.1	0.5	2.4	0.4	2.044	674.8
		22	4.1	0.6	95	5	5.0	0.3	12.4	0.5	3.0	0.5	2.044	670.6

		42	3.5	0.5	87	4	12.7	0.6	16.0	0.5	4.5	0.7	2.046	664.7
		62	5.0	0.7	86	4	13.8	0.7	18.5	0.6	3.7	0.6	2.046	660.8
		93	6.1	0.9	79	4	21	1	21.4	1.0	3.5	0.6	2.046	658.3
		214	9	1	93	5	6.8	0.3	24.3	0.8	2.7	0.4	2.049	649.9
		333	11	2	85	4	15.0	0.8	27	2	2.4	0.4	2.053	642.9
		361	12	2	87	4	12.7	0.6	25	1	2.1	0.3	2.054	--
M22	$[HClO_4] = 10^{-2}$ mol L^{-1}	0	0	0	--	--	--	--	0	0	--	--	--	--
		360	10	2	--	--	--	--	16.1	0.9	1.5	0.2	--	--
		727	17	3	--	--	--	--	21	1	1.2	0.2	--	--
		1507	26	4	--	--	--	--	34	2	1.3	0.2	--	--

Table 3: Analytical results for runs in [HCl] = $10^{-1.5}$ and 10^{-2} mol L^{-1} and [$HClO_4$] = 10^{-3} mol L^{-1} media.

Run	Medium	Time	[Fe]	σ	$Fe^{(II)}$	σ	$Fe^{(III)}$	σ	[SO_4^{2-}]	σ	R	σ	pH	Eh
		min	*µmol L^{-1}*		*(%)*				*µmol L^{-1}*					*MV/ESH*
M05	[$HClO_4$] = 10^{-3} mol L^{-1}	0	0	0	--	--	--	--	0	0	--	--	2.998	644.4
		5	0.5	0.2	54	3	46	2	13	2	26	11	3.025	628.3
		27	1.5	0.1	100	5	0	0	20.9	0.8	14	1	3.112	601.4
		52	1.9	0.1	100	5	0	0	27.5	1	14.5	0.9	3.091	593.3
		72	2.39	0.07	79.97	4.00	20.03	1.00	18.4	0.7	7.7	0.4	3.077	591.1
		94	2.6	0.1	100	5	0	0	37.3	0.9	14.3	0.7	3.062	590.5
		124	3	0.2	100	5	0	0	51	2	17.0	1.3	3.037	590.6
		169	3.4	0.2	82.6	4.1	17.4	0.9	53	2	16	1	3.045	--
		231	3.6	0.1	75	4	25	1	57	5	16	1	--	--
		298	4.2	0.1	81.4	4.1	18.7	0.9	68	1	16.2	0.5	--	--
		357	4.7	0.2	76	4	24	1	69	1	14.7	0.7	--	606.7
		471	5.5	0.3	88.7	4.4	11.3	0.6	85	2	15.5	0.9	--	600.9
M13	[HCl] = 10^{-2} mol L^{-1}	0	0	0	--	--	--	--	0	0	--	--	2.014	673.2
		5	1.9	0.3	--	--	--	--	8	1	4	0.8	2.012	629.2
		20	4.6	0.7	--	--	--	--	11	2	2.4	0.5	2.002	641.7
		40	4.9	0.7	--	--	--	--	12	2	2.3	0.6	2.004	645.8
		60	5.2	0.8	--	--	--	--	11.5	1.0	2.2	0.4	2.006	648.5
		90	6.4	1.0	--	--	--	--	13	1	2.0	0.3	2.007	645.1
		150	7	1	--	--	--	--	13	1	1.763	0.300	2.009	638.6
		180	8	1	--	--	--	--	13.4	1.0	1.6	0.3	2.011	638.0
		270	9	1	--	--	--	--	13	1	1.5	0.3	2.014	638.2
		365	10	2	--	--	--	--	16.3	1.0	1.6	0.3	2.016	639.0
M19	[$HClO_4$] = 10^{-3} mol L^{-1}	0	0	0	--	--	--	--	0	0	--	--	3.057	676.9

		5	1.5	0.2	--	--	--	--	7	2	4	1	3.062	639.8
		20	2.3	0.3	--	--	--	--	7	2	3.3	0.9	3.052	632.0
		40	3.5	0.5	--	--	--	--	8	2	2.4	0.6	3.068	626.5
		60	3.7	0.6	--	--	--	--	9	2	2.4	0.6	3.083	626.4
		90	5.2	0.8	--	--	--	--	10	2	2.0	0.4	3.080	627.4
		180	6.69	1.00	--	--	--	--	11	2	1.7	0.3	3.090	622.3
		274	8	1	--	--	--	--	12	2	1.48	0.30	3.089	616.1
		360	9	1	--	--	--	--	12	2	1.3	0.3	3.094	612.4
M21	[HCl] = $10^{-1,5}$ mol L^{-1}	0	0	0	--	--	--	--	0	0	--	--	1.577	736.6
		5	4.6	0.5	1.9	0.1	98	5	6	2	1.2	0.4	1.575	670.0
		20	6.2	0.6	22	1	78	4	8	2	1.3	0.3	1.579	659.7
		40	6.7	0.7	8.5	0.4	91	5	8	2	1.1	0.3	1.583	655.6
		60	7.7	0.8	0	0	100	5	8	2	1.1	0.3	1.592	653.1
		90	7.8	0.8	1.8	0.1	98	5	13	2	1.7	0.3	1.600	651.6
		120	7.7	0.8	2.0	0.1	98	5	9.7	2.0	1.3	0.3	1.606	650.2
		180	8.7	0.9	0.0	0	100	5	12	2	1.4	0.3	1.631	647.0
		270	9.5	0.9	9.9	0.5	90	5	10	2	1.1	0.2	1.644	640.9
		360	9.8	1.0	15.7	0.8	84	4	11.8	2.0	1.2	0.2	1.665	637.3

Table 4: Ratios $R = [SO_4^{2-}]/[Fe]_{tot}$ calculated from data taken from Ichikuni (1960), McKibben and Barnes (1986) and Bonnissel-Gissinger et al. *(1998).*

pH	Medium	R announced	R calculated	Reference
1.1	HCl 10^{-1} mol L^{-1}	0.67	0.74 ± 0.02	Ichikuni (1960)
1.89	HCl + H_2O_2	--	1.3 ± 0.1	McKibben and Barnes (1986)
2	HCl 10^{-2} mol L^{-1}	1.57	1.38 ± 0.05	Ichikuni (1960)
2.5	HNO_3	--	1.6 ± 0.2	Bonnissel-Gissinger *et al.* (1998)
2.9	HCl 10^{-3} mol L^{-1}	2.7	1.92 ± 0.07	Ichikuni (1960)
3.2	H_2O	4.78	2.8 ± 0.1	Ichikuni (1960)

Table 5: Ratios $[SO_4^{2-}]/[Fe]_{tot}$ (R) inferior or equal to 2 in function of $S^{(n)}$ and $S^{(n')}$ ($0 < n < n'$ and $n' \leq 6$) inherited from the pyrite oxidation with a disproportion step into S^0; ΔG_R of the disproportion step is also indicated (in kJ mol^{-1}). See Descostes (2001) for thermodynamic data.

$S^{(n)}$	n	$S^{(n')}$	n'	ΔG_R	R
$S_2O_3^{2-}$	2	$S_4O_6^{2-}$	2,5	-36.0	1.60
		$S_3O_6^{2-}$	10/3	-3.1	1.20
		SO_2	4	-14.9	1.00
		$S_2O_6^{2-}$	5	-6.4	0.8
		SO_4^{2-}	6	-58.8	0.67
$S_5O_6^{2-}$	2	$S_4O_6^{2-}$	2.5	-82.4	1.60
		$S_3O_6^{2-}$	10/3	0.0	1.20
		SO_2	4	-29.6	1.00
		$S_2O_6^{2-}$	5	-8.4	0.8
		SO_4^{2-}	6	-124.3	0.67
$S_4O_6^{2-}$	2.5	SO_4^{2-}	6	-41.9	0.83
$S_2O_4^{2-}$	3	$S_3O_6^{2-}$	10/3	-70.2	1.8
		SO_3^{2-}	4	-11.6	1.5
		SO_2	4	-88.0	1.5
		$S_2O_5^{2-}$	4	-52.8	1.5
		$S_2O_6^{2-}$	5	-75.2	1.2
		SO_4^{2-}	6	-144.7	1
$S_3O_6^{2-}$	10/3	SO_2	4	-29.6	1.67
		$S_2O_6^{2-}$	5	-8.4	1.33
		SO_4^{2-}	6	-124.3	1.11
SO_3^{2-}	4	$S_2O_6^{2-}$	5	-42.4	1.6
		SO_4^{2-}	6	-88.7	1.33
SO_2	4	SO_4^{2-}	6	-37.9	1.33
$S_2O_5^{2-}$	4	$S_2O_6^{2-}$	5	-29.9	1.60
		SO_4^{2-}	6	-122.6	1.33
$S_2O_6^{2-}$	5	SO_4^{2-}	6	-115.9	1.67

FIGURES

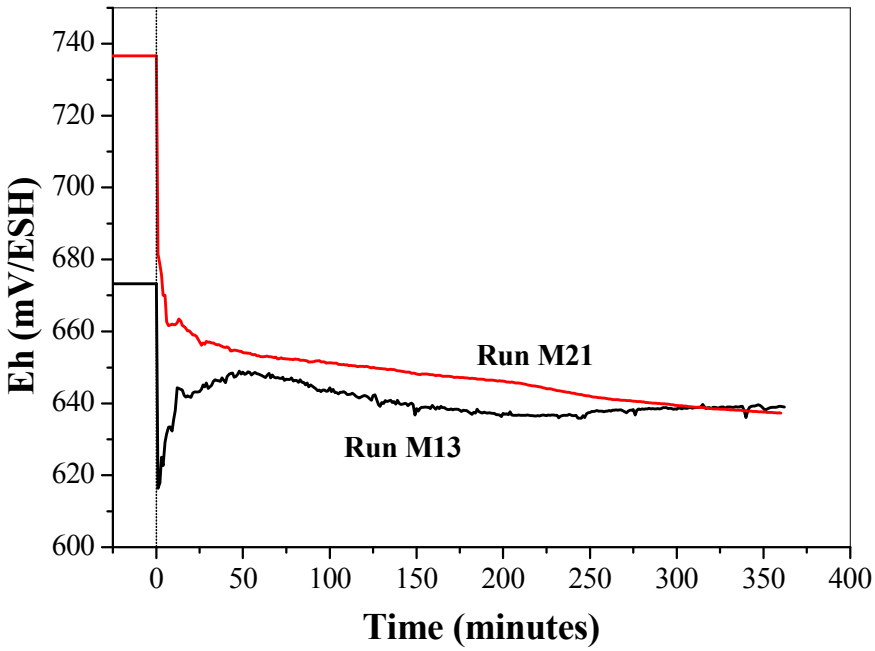

Figure 1: Comparison of redox potential (Eh) trends in [HCl] = 10^{-2} mol L^{-1} (run M13) and [HCl] = $10^{-1.5}$ mol L^{-1} (run M21) media.

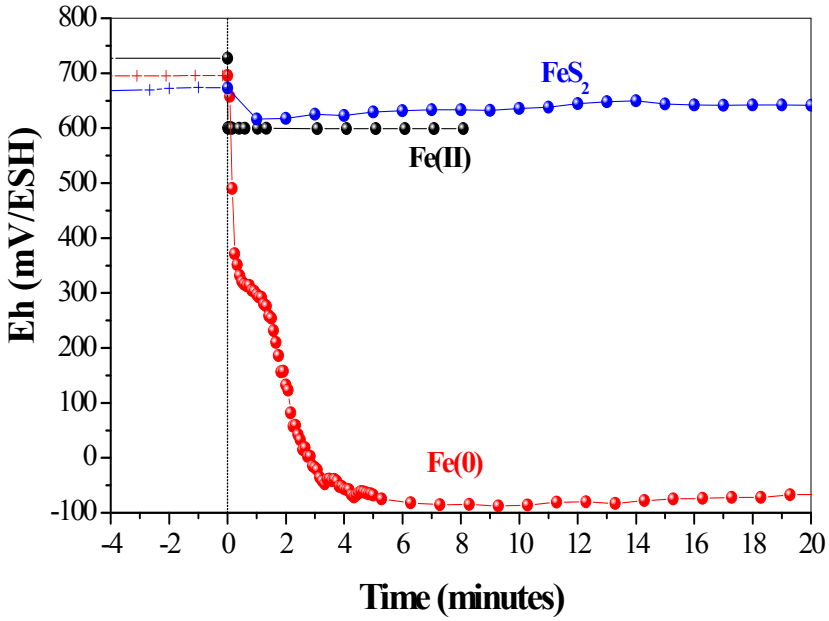

Figure 2: Eh trends in [HCl] = 10^{-2} mol L^{-1} medium for different iron oxidation number.

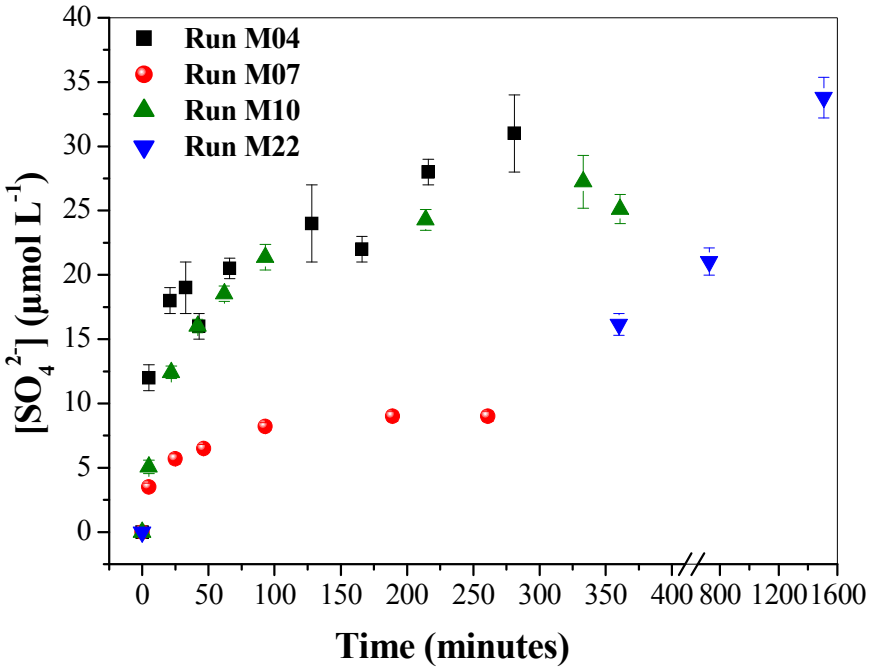

A

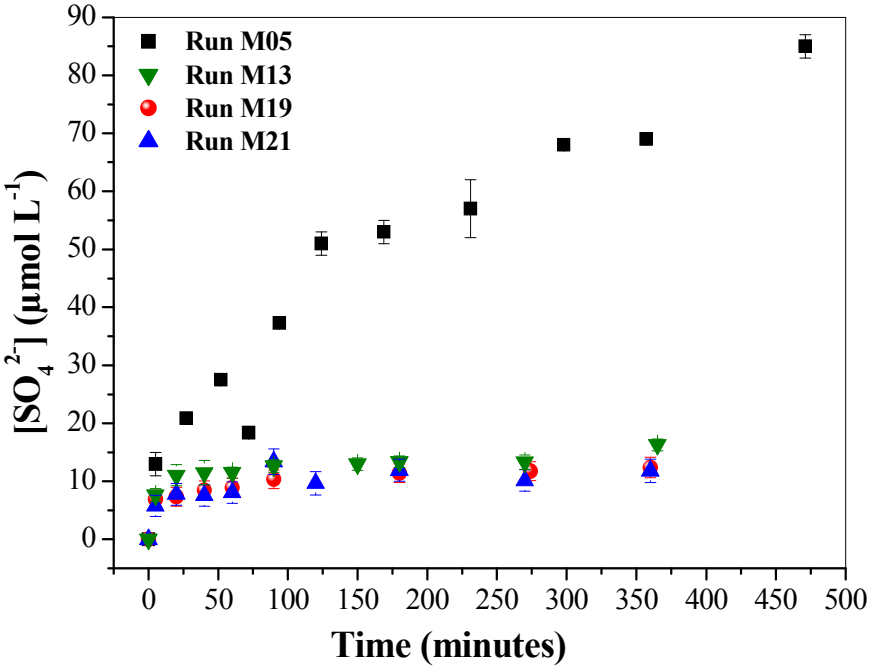

B

*Figure 3: Comparison of sulphate contents trends (**A**: [$HClO_4$] = 10^{-2} mol L^{-1} – runs M04, M07, M10 and M22; **B**: [HCl] = $10^{-1.5}$ mol L^{-1} – run M21, [HCl] = 10^{-2} mol L^{-1} – run M13 [$HClO_4$] = 10^{-3} mol L^{-1} – runs M05 and M19).*

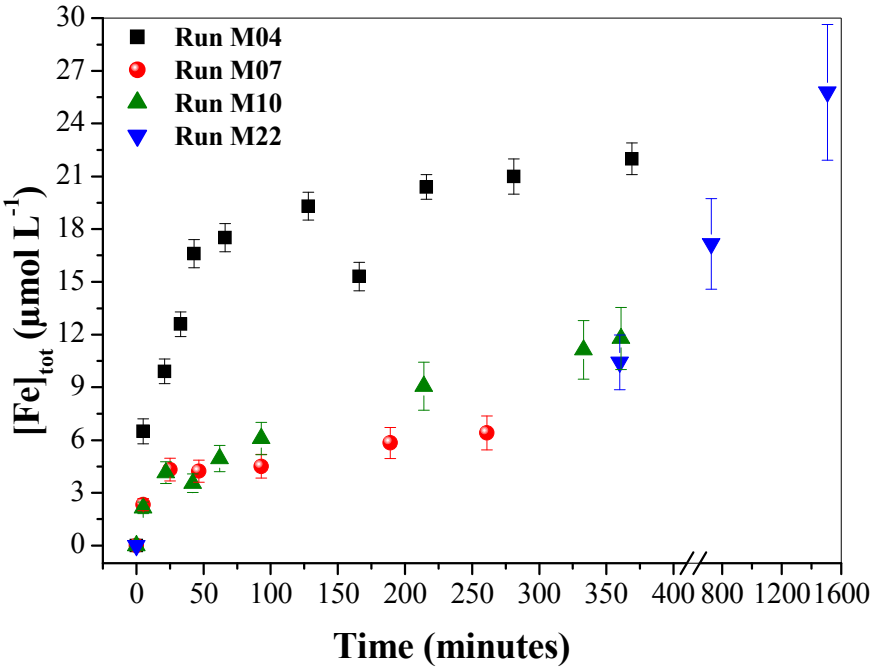

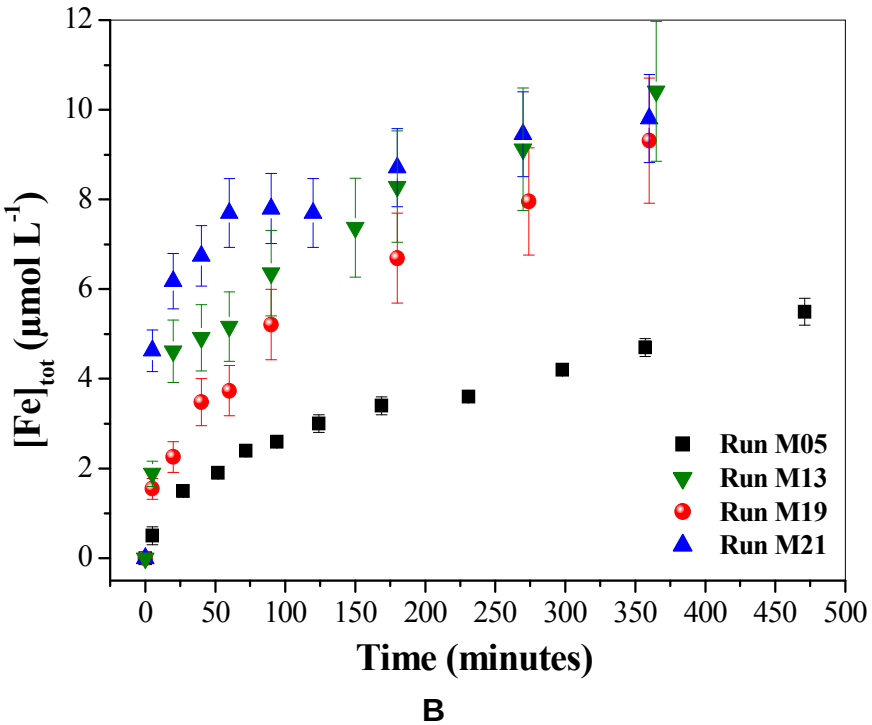

*Figure 4: Comparison of iron contents trends (**A**: [$HClO_4$] = 10^{-2} mol L^{-1} – runs M04, M07, M10 and M22; **B**: [HCl] = $10^{-1.5}$ mol L^{-1} – run M21, [HCl] = 10^{-2} mol L^{-1} – run M13 [$HClO_4$] = 10^{-3} mol L^{-1} – runs M05 and M19).*

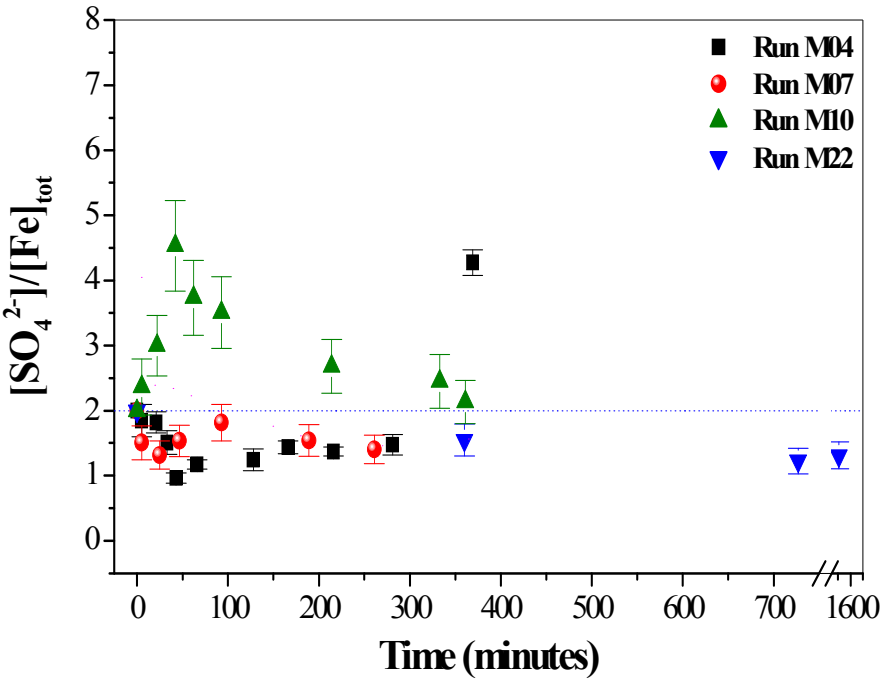

A

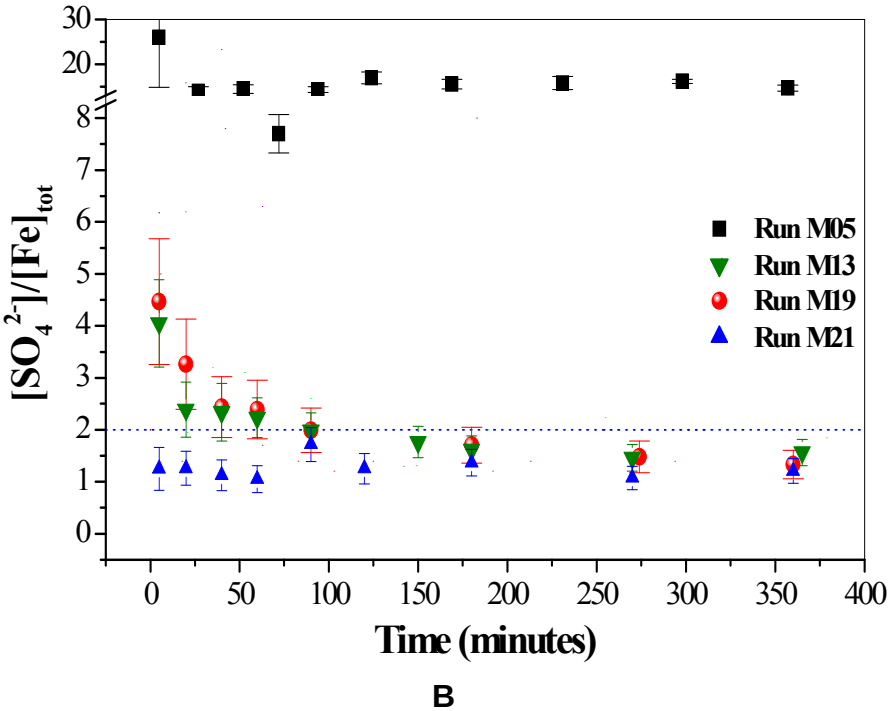

B

*Figure 5: Comparison of ratios R = $[SO_4^{2-}]/[Fe]_{tot}$ trends (**A**: $[HClO_4] = 10^{-2}$ mol L^{-1} – runs M04, M07, M10 and M22; **B**: $[HCl] = 10^{-1.5}$ mol L^{-1} – run M21, $[HCl] = 10^{-2}$ mol L^{-1} – run M13 $[HClO_4] = 10^{-3}$ mol L^{-1} – runs M05 and M19).*

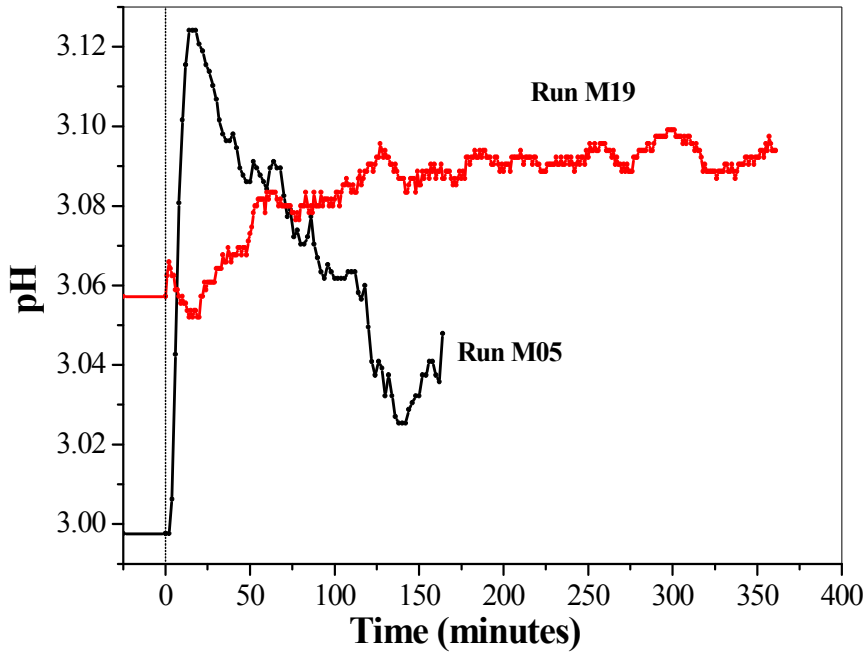

Figure 6: Comparison of pH trends in [$HClO_4$] = 10^{-3} mol L^{-1} medium (runs M05 and M19).

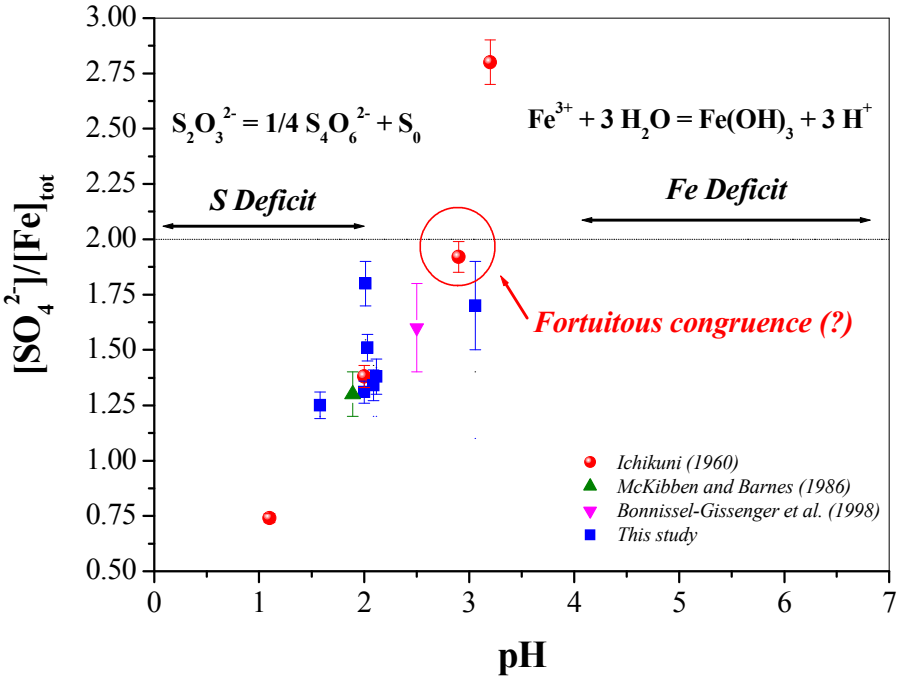

Figure 7: Comparison of ratios R = [SO_4^{2-}]/[Fe]$_{tot}$ calculated in this study and from data taken from literature.

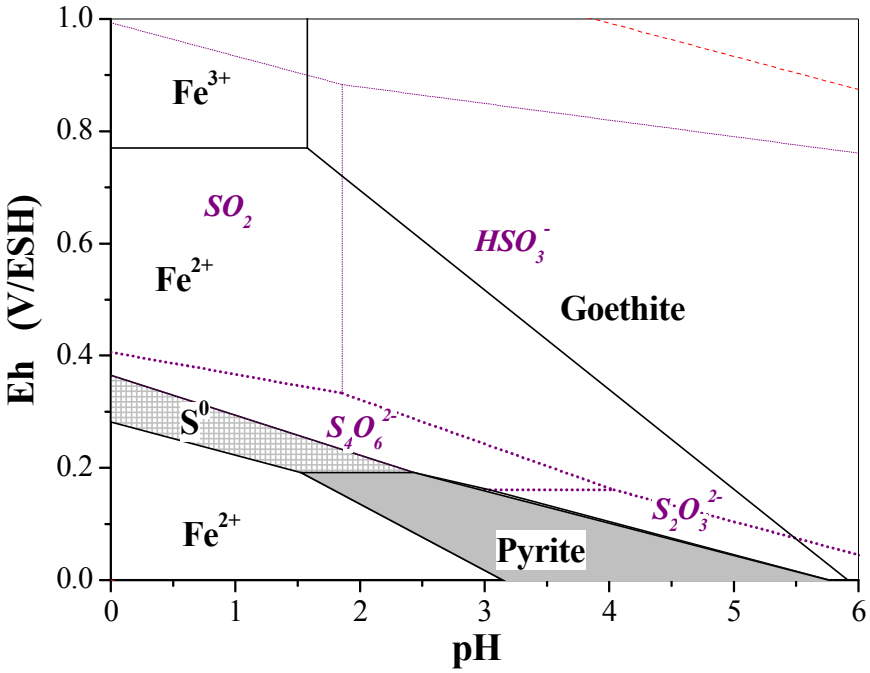

Figure 8: Eη–πH διαγραμ φορ συλπηυρ – ιρον – ωατερ σψστεμ ατ 25°X, χονσιδερινγ ον λψ συλπηυρ σπεχιεσ ωιτη αν οξιδατιον νυμβερ ινφεριορ το συλπηατε ([ΣS] = 2 × [ΣFe] = 2.10^{-5} mol L^{-1}). See Descostes (2001) for thermodynamic data.